MICROSTRUCTURE AND TEXTURE EVOLUTION OF PURE MAGNESIUM DURING ECAE

Somjeet Biswas, Satyaveer Singh D., Satyam Suwas[ξ]
Laboratory for Texture and Related Studies, Department of Materials Engineering, Indian Institute of Science, Bangalore -560012, India

Keywords: Equal Channel Angular Extrusion (ECAE), Texture, Microstructure, Electron Back Scattered Diffraction (EBSD), Discontinuous Dynamic Recrystallization (DDRX)

Abstract

Initially hot rolled commercially pure magnesium and having a basal texture was deformed by Equal Channel Angular Extrusion (ECAE). ECAE was carried out up to 4 passes in a 90° die following three different routes (A, B_c and C) at a temperatures of 523 K. Systematic analysis of microstructures, grain size distributions, texture and grain boundary character distributions was carried out using electron back scattered diffraction in field emission gun scanning electron microscope in the transverse plane. In addition to significant reduction in grain size, strong <0002> fiber texture inclined at an angle ~ 45° from the extrusion axis formed in the material. Texture was also analyzed by orientation distribution function (ODF) and compared vis-à-vis shear texture. A significant amount of dynamic recrystallization occurred during ECAE, which apparently did not influence the deformation texture.

Introduction

Magnesium alloys have very high potential to be used in automobile, aerospace and electronics industries because of their lowest density amongst the structural materials and significant reduction in weight [1]. The application potentials are, however, impeded by poor formability consequent to its limited ductility at room temperature which is attributed to the hexagonal closed packed (h.c.p.) crystal structure of magnesium having limited slip systems. In order for magnesium alloys to be a viable industrial material, an appropriate tailoring of microstructure is necessary. Conventional processing of magnesium involves deformation at relatively higher temperature; therefore, grain sizes cannot be reduced beyond a certain extent. Moreover, all such processing methods lead to the development of textures that are not suitable for further processing. Amongst several alternatives, equal channel angular extrusion (ECAE) process, where the deformation mode is near simple shear and requires a fewer number of slip systems, is very effective in enhancing the workability and strength of Mg alloys [2-4]. Incidentally, this process leads to texture suitable for further plastic deformation [5-8]. The improvement in mechanical behavior of ECAE processed Mg and its alloys make the process more attractive for engineering applications [9-11].

The ECAE process consists of extruding a well lubricated billet through two channels of equal and identical area of cross section. The process can be repeated multiple-times without any change in the area of cross section of the specimen. As a result of this, large plastic deformation with constant change in strain path can be imparted in the course of multi-pass ECAE, leading to ultrafine grain sizes as well as characteristic texture.

A rigorous analysis of texture formed in ECAE processed magnesium on the basis of ideal orientation developed in simple shear was carried out by Beausir et al. [12,13]. The present study was undertaken to explore the possibility of grain refinement and the associated texture development.

Experimental

The initial material was hot rolled commercially pure magnesium having strong basal texture. Keeping the RD (rolling direction), ND (normal direction) and TD (transverse direction) into account, rods of square cross section with the dimension 10 mm X 10 mm X 100 mm were extracted from this plate. The rods were deformed in an ECAE die with inter-channel angle 90° without rounding of corners, where an effective strain of 1.17 per pass could be imparted [14]. The rods were well lubricated and then inserted in the ECAE die with the ND in the front and the RD down (Fig. 1). ECAE was carried out following the routes by A, B_C and C up to 4 passes at 523 K. The billets were preheated at 523 K for 10 minutes before entering the first channel of the die through the inlet.
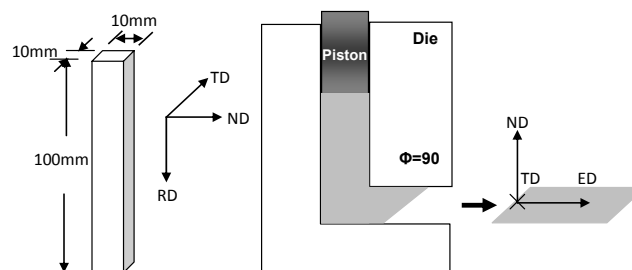

Figure 1. Schematic of Equal channel Angular Extrusion

Microstructure, grain size distribution, grain boundary character distribution and quantitative texture evolution using (002), (10$\bar{1}$0) and (11$\bar{2}$0) Pole Figures and orientation distribution function (ODFs) were carried out by Electron back scattered diffraction (EBSD) analysis done on Field Emission Gun - Scanning Electron Microscope (FEG-SEM). EBSD was performed by cutting the samples along the ED-ND plane, preserving the ED, ND and TD. The data processing was carried out with TSL software.

[ξ] email : satyamsuwas@materials.iisc.ernet.in

Evolution of Microstructure

The initial microstructure and the microstructures after ECAE is shown in Fig. 2 through inverse pole figure (IPF) maps.
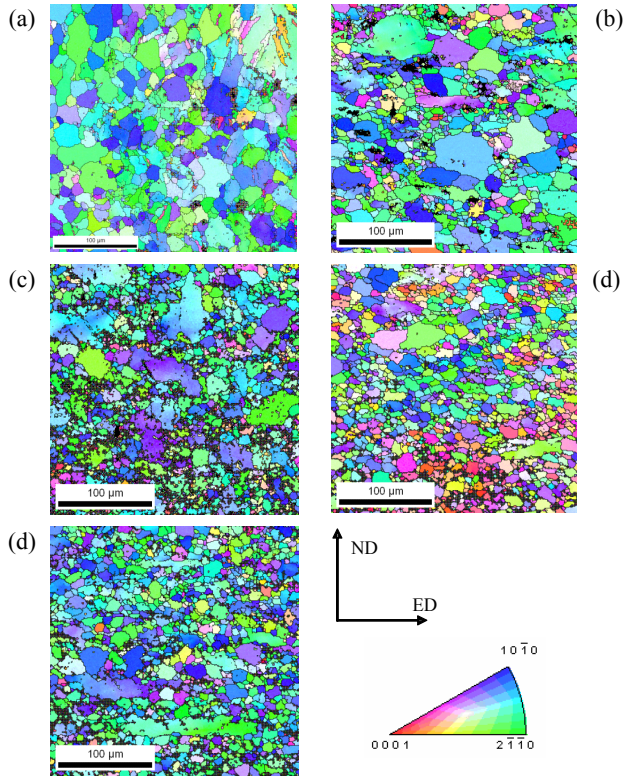
(a) (b)

(c) (d)

(d)

ND

ED

$10\bar{1}0$

0001 $2\bar{1}\bar{1}0$

Figure 2. Inverse Pole Figure (IPF) Maps of (a) Starting Material (b) 1 Pass, (c) 4A, (d) 4B$_C$, (e) 4C

Table 1 shows the average grain size of the initial and the ECAE processed samples as determined by linear intercept method.

Table 1. Average grain size (μm) of initial and all the ECAE processed samples

Grain Size in (μm)	Starting Material	1 Pass	4A	4B$_C$	4C
21.1		5.9	6.18	5.89	6.21

The average grain size of the initial material was ~ 21 μm. After 1 pass of ECAE, the grain size reduced to ~ 6 μm. After deformation to 4 passes by routes A, B$_C$ and C a similar grain size was obtained.

Fig. 3 represents the grain size distribution of the initial and the ECAE processed samples after 1 pass and 4 pass by routes A, B$_C$ and C. Grain size distribution was almost found to have a singular peak.

To see the grain boundary character distribution (GBCD) of the initial, 1 pass and 4 pass ECAE processed samples, misorientation angle distributions were plotted in Fig. 4. The distribution is clearly bimodal with a large fraction of low angle grain boundaries (LAGBs). A comparison of relative fraction of low and high angle boundaries (HAGBs) was conducted. The fraction of LAGBs was ~ 0.65 for the initial material; it decreases to ~0.5 after 1 pass. After 4 passes, the LAGBs decreases to ~0.35 for route A, ~0.31 for route B$_C$ and ~0.32 for route C. In addition to a detailed misorientation angle distribution described above, the extent of twinning was estimated from the analysis of EBSD data. The measurement of $\{10\bar{1}2\}$ tensile twin boundaries ($86^o \pm5^o$ $\langle11\bar{2}0\rangle$), $\{10\bar{1}1\}$ compression twin boundaries ($56^o \pm5^o$ $\langle11\bar{2}0\rangle$, $\{10\bar{1}1\}\_\{10\bar{1}2\}$ double twinning ($38^o \pm5^o$ $\langle11\bar{2}0\rangle$) was carried out. It was found that for all the ECAE processed samples the fraction of twin boundary was almost negligible. A maximum of ~0.03 of tensile twins present after 1 pass, which reduces to ~0.02 after 4 passes for all the three routes.

A detailed analysis of microstructures as recorded through IPF (Fig. 2) reveals the presence of fine equiaxed grains with serrated grain boundaries. The smaller equiaxed grains surrounding the bigger grains in all the ECAE samples indicate that discontinuous dynamic recrystallization (DDRX) has taken place. This could be due to relatively high temperature of deformation. It is to be noted that the minimum recrystallization temperature for pure magnesium should be ~373K. In order to visualize this effect in a more appreciable way, misorientation angle distributions for all the ECAE processed samples were plotted (Fig. 3). A bimodal distribution with the decrease in LAGBs for all the routes also indicates the same.

Evolution of Texture

Figure 5 shows the (0002), $(10\bar{1}0)$, and $(11\bar{2}0)$ pole figures of the starting material, 1 pass and 4 pass ECAE processed samples for routes A, B$_C$ and C as measured on ED-ND plane. The starting material showed a strong non-axisymmetric (0002) basal texture with the fiber axis parallel to the extrusion direction (ED). After 1st pass, basal poles rotate around the axis TD, and tend to approach the ideal B fiber position (which lies in the 45° intersection plane of the die). A split of the fiber could be seen in the (0002) pole figure.

The basal pole rotates around TD after each pass. However, even after 4th pass by route A, it cannot reach the B fiber position. The texture after 1 pass and 4 pass route A remained almost same with the same texture intensity (~8 MRD (Maximum random distribution) in case of basal pole) but the split in the basal texture is not present.
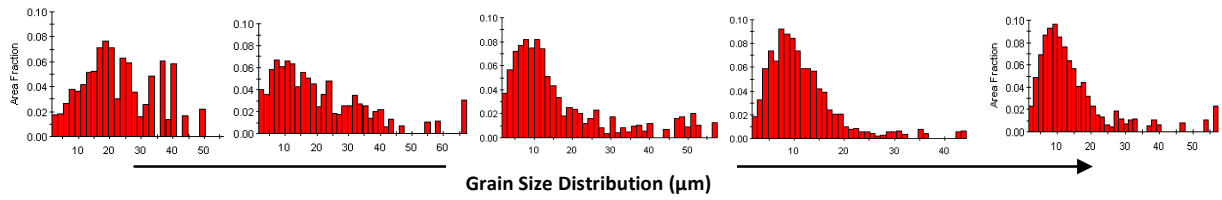
Figure 3. Grain Size Distribution of (a) Starting Material, (b) 1 Pass, (c) 4A, (d) 4B$_C$ and (e) 4C
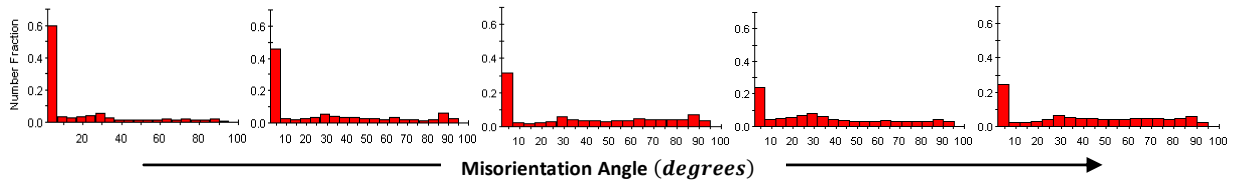

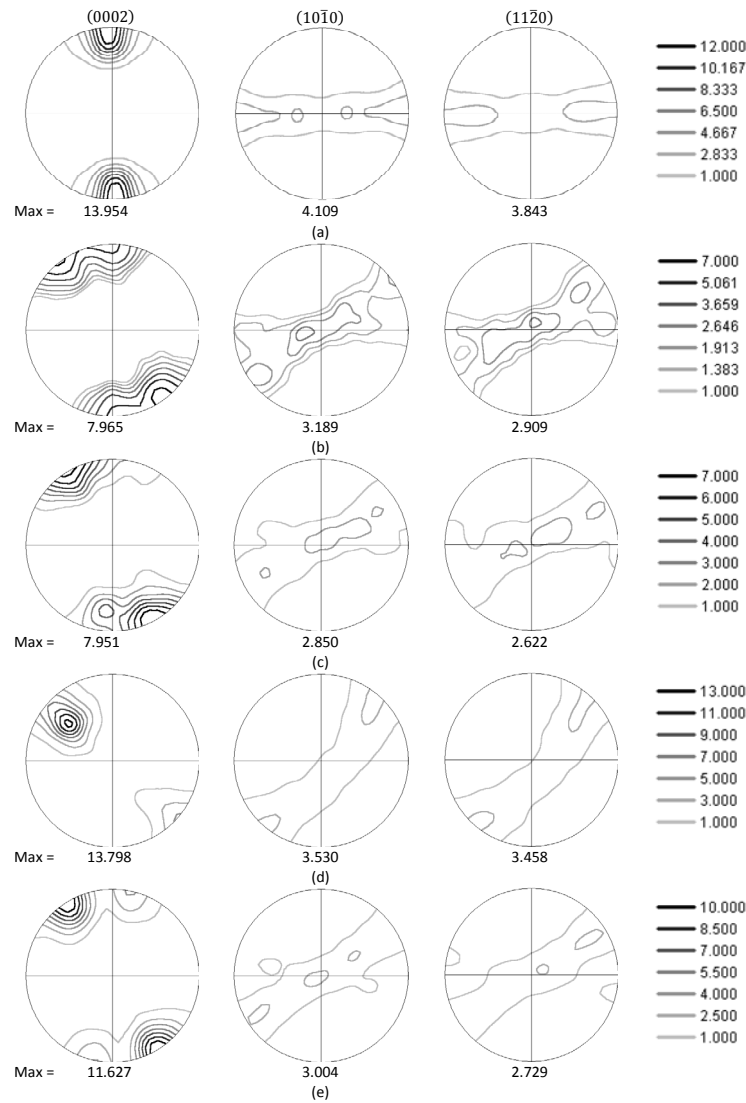Figure 4. Misorientation Angle Map of (a) Starting Material, (b) 1 Pass, (c) 4A, (d) 4B$_C$ and (e) 4C

Figure 5. (0002), (10$\bar{1}$0) , and (11$\bar{2}$0) Pole Figures of (a) Starting Material (b) 1 Pass, (c) 4A, (d) 4B$_C$, (e) 4C

The texture development in the 4th pass Route B_C displays a systematic difference from route A and route C which is clearly visible in the (0002) pole figures; namely, the B fiber develops in a slightly *rotated* position around an axis with an intensity of ~14 MRD. The texture has no symmetry. Route B_C is distinct as the texture rotates by a much smaller amount and not around the TD axis.

In case of 4 passes by route C, a split in the fiber can be noticed in the (0002) pole figure same as after 1 pass. The texture is almost same as after the 4th pass through route A with a higher texture intensity of ~12 MRD.

The intensity of basal pole is always higher than that of the prismatic poles in all the cases.

A detailed analysis of texture was carried out by the method of orientation distribution function (ODF). The $\varphi_2 = 0$ and 30° of

the initial, 1st pass and the 4th pass ECAE processed samples are shown in Fig. 6 (a), (b), (c), (d) and (e). It can be observed that the texture of all the ECAE samples consists of the same fibers B and C_2, slightly rotated from their ideal positions. Except in case of route B_C, where the C_2 fiber is absent. The ideal positions of various fibers are shown in Fig. 6 (f). It can be seen that the strength of texture fibers *f(g)* decreases after 1 pass to ~ 13.3. For route A, the *f(g)* decreases at 4th pass to ~ 10.3. For B_C route the *f(g)* increases after 4th pass to ~15.5. In case of route C after 4th pass, the texture intensity remained almost same as the 1st pass.

Though a significant degree of DRX took place during ECAE, the texture fibers almost matches the ideal orientations shown in Table1, which indicates the fact that in magnesium, dynamic recrystallization does not alter the deformation texture
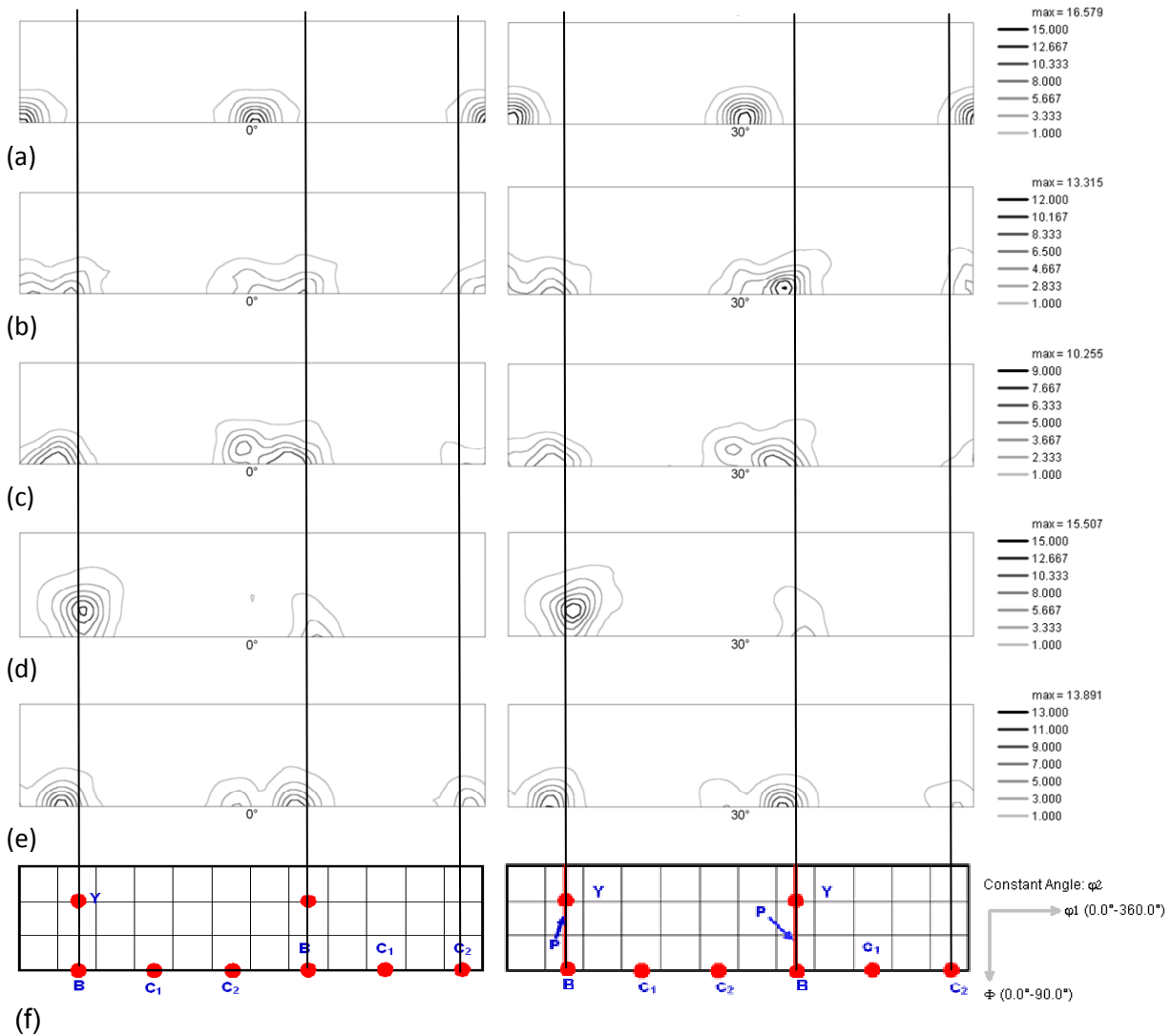

Figure 6. $\varphi_2 = 0$ and $\varphi_2 = 30$ ° Section of the Orientation Distribution Functions (ODFs) of (a) Starting Material (b) 1 Pass, (c) 4A, (d) 4B_C, (e) 4C and (f) Ideal orientations

Summary and Conclusions

The formation of equiaxed and serrated grains as well as bimodal misorientation angle distribution indicates discontinuous dynamic recrystallization (DDRX) occurs in Magnesium during ECAE. Texture developed after each ECAE pass for route A and C is almost similar and a rotated B and C_2 fiber develops. While texture after processing from route B_C is characterized by an asymmetric B fiber formed at a rotated position, with no trace of C_2 fiber. Dynamic recrystallization in magnesium does not alter the deformation texture.

Acknowledgement

References

1. Stalmann, W. Sebastian, H. Friedrich, S. Schumann, K. Dröder, *Adv. Engg. Mater.*, 3 (2001) 969.
2. M. Mabuchi, K. Ymeyama, H. Iwasaki, K. Higashi, *Acta Mater.*, 47 (1999) 2047.
3. S. Komodo, T. Ashie, H. Yamada,K. Sanbun, Y. Kojima, *Mater. Sci. Forum*, 65 (2000) 350.
4. S. R. Agnew, G. M. Stoica, Li Chen, T. M. Lillo, J. Macheset, P.K. Liaw, In: Y. T. Zhu et al. Editors, *Ultra fine grain Materials II*, Warrendale, PA: TMS, 2002, 643.
5. T. Mukai, M. Yananoi, H. Watanabe, K. Higashi, *Scripta Mater.*, 45 (2001) 89.
6. W. J. Kim, C. W. An, Y. S. Kim, S. I. Hong, *Scripta Mater.*, 47 (2002) 39.
7. T. Mukai, Y. Masashi, K. Iligashi, Mater. *Trans. JIM*, 42 (2001) 2652.
8. S. Suwas, G. Gottstein., R. Kumar, *Mater. Sci. Engg. A* , 471(1-2) (2007) 1-14
9. S. R. Agnew, P. Mehrotra, T.M. Lillo, G.M. Stoica, P.K. Liaw, *Mater. Sci. Engg. A*, 408 (2005) 72.
10. S. R. Agnew, J. A. Horton, T. M. Lillo, D. W. Brown, *Scripta Mater.*, 50 (2003) 377.
11. S. R. Agnew, P. Mehrotra, T.M. Lillo, G.M. Stoica, P.K. Liaw, *Acta Mater.*, 53 (2005) 3135.
12. B. Beausir, L.S. Tóth, K.W. Neale *Acta Mater.,* 55 (2007) 2695-2705.
13. B. Beausir, S. Suwas, L.S. Tóth, K.W. Neale, J.-J. Fundenberger, *Acta Mater.,* 56 (2008) 200-214.
14. J.-P. Mathieu, S. Suwas, A. Eberhardt, L.S. Toth, P. Moll, *J. Mater. Proc. Tech..*, 173 (2006) 29-33.
15. M. Farukawa, Y. Iwashashi, Z Horita, M. Nemoto, T. G. Langdon, *Mater. Sci. Engg., A*, 257 (1998) 328.